Available online at www.sciencedirect.com
SCIENCE DIRECT®
Phytochemistry 66 (2005) 113–124
PHYTOCHEMISTRY
www.elsevier.com/locate/phytochem

Isolation and structural identification of diarabinosyl 8-*O*-4-dehydrodiferulate from maize bran insoluble fibre

Ella Allerdings [a], John Ralph [b,c], Paul F. Schatz [b], Diana Gniechwitz [a], Hans Steinhart [a], Mirko Bunzel [a,*]

[a] *Department of Food Chemistry, Institute of Biochemistry and Food Chemistry, University of Hamburg, Grindelallee 117, 20146 Hamburg, Germany*
[b] *US Dairy Forage Research Center, USDA Agricultural Research Service, Madison, WI 53706, USA*
[c] *Department of Forestry, University of Wisconsin, Madison, WI 53706, USA*

Received 16 July 2004; received in revised form 18 October 2004
Available online 8 December 2004

Abstract

The first saccharide ester of a dehydrodiferulic acid (DFA) other than 5-5-DFA has been isolated from maize bran insoluble fibre after acidic hydrolysis and fractionation by gel chromatography and semi-preparative RP-HPLC. HPLC-MS along with 1D, 2D and 3D NMR spectra provided the requisite structural evidence that it is the di-5-*O*-L-arabinosyl ester of 8-*O*-4-DFA. Although a range of DFAs have been well authenticated as components released from the cell walls of grasses, the only structural evidence for a DFA attached to polysaccharides had been from 5-5-DFA. The isolation of the 8-*O*-4-ester demonstrates that polysaccharides in maize cell walls, and presumably in all grasses, are cross-linked through dehydrodiferulates other than 5-5-dehydrodiferulate.

Keywords: Zea mays L.; Graminaceae; Maize bran; Ferulic acid dehydrodimers; Diferulates; Polysaccharides; Cell wall cross-linking; NMR

1. Introduction

Ferulic acid is incorporated into plant cell walls of various monocots and some dicots (Ishii, 1997). Ferulates are most predominant within species of the Gramineae, maize bran being an especially rich source (Bunzel et al., 2001). In most grasses ferulic acid is ester-linked at the C-5 position to α-L-arabinosyl residues of arabinoxylans, whereas in dicots it is primarily linked to pectins (Ishii, 1997). Because they can act as cross-linking agents between polysaccharides, or between polysaccharides and lignin (Ralph et al., 1994, 1995, 1998), ferulates modify the mechanical properties of cell walls (Eraso and Hartley, 1990; Grabber et al., 1998a,b; Kamisaka et al., 1990; Tan et al., 1992; Zarra et al., 1999), and affect forage cell wall digestibility by ruminants (Deetz et al., 1993; Grabber et al., 1998a,b). The degree of ferulate cross-linking between pectic polysaccharides is conjectured to have a role in maintaining crispness of vegetables after cooking since it affects the thermal stability of cell–cell adhesion and, therefore, texture in tissues (Waldron, 1998; Waldron et al., 1997). Cross-linking of cell wall polysaccharides by ferulates may influence the physico-chemical behaviour of dietary fibre and may affect its physiological properties, e.g. bulk, fermentability, binding and adsorptive capacity (Bunzel et al., 2001).

The predominant mechanism for cross-linking cell wall polysaccharides is ferulate dehydrodimerisation via radical coupling (Ralph et al., 1994). Dehydrodiferulates have been identified and quantified in various plant materials and are characterised as 8-5-, 5-5-,

* Corresponding author. Tel.: +49 40 42838 4379; fax: +49 40 42838 4342.
E-mail address: mirko.bunzel@uni-hamburg.de (M. Bunzel).

0031-9422/$ - see front matter © 2004 Elsevier Ltd. All rights reserved.
doi:10.1016/j.phytochem.2004.10.026

8-8-, 8-*O*-4-, and 4-*O*-5-coupled dehydrodimers (Bunzel et al., 2000, 2001; Parr et al., 1996, 1997; Ralph et al., 1994; Saulnier and Thibault, 1999). However, these studies are limited to the identification of dehydrodiferulic acids released following saponification. Evidence for polysaccharide cross-linking via dehydrodiferulates is possible by isolation and identification of feruloylated saccharide fragments. The isolation of dehydrodiferulates linked to carbohydrates has been reported only from bamboo shoots following enzymatic hydrolysis (Ishii, 1991) and from maize bran following acidic hydrolysis of cell walls (Saulnier et al., 1999). This provided the first structural evidence that ferulate dehydrodimerisation products cross-link saccharide units in the cell wall polysaccharides. However, in both cases, only 5-5-diferuloyl saccharides have been isolated.

The isolation of 5-5-diferuloyl oligosaccharides, however, does not prove intermolecular cross-linking between two different polysaccharide chains. Molecular modelling experiments suggested that the 5-5-linked diferulate is unique in that it could be formed intramolecularly (Hatfield and Ralph, 1999). This intramolecular coupling is possible when arabinose residues bearing ferulate units are positioned three xylose residues apart on the same xylan chain (Hatfield and Ralph, 1999). The recent isolation and identification of a 5-5/8-*O*-4-coupled dehydrotriferulic acid from maize cereal grain was suggested to result from initial intramolecular 5-5-dehydrodimerisation followed by intermolecular coupling of the resulting 5-5-dehydrodiferulate (at one of its 8-positions) with ferulate on another chain (at its 4-*O*-position), rather than the interaction of three ferulates on three separate chains (Bunzel et al., 2003). At essentially the same time, another research group identified the same trimer and also concluded that the cross-linking nature of the trimer remained unknown (Rouau et al., 2003).

In this paper, we describe the isolation and the structural identification of the di-5-*O*-L-arabinosyl ester of 8-*O*-4-dehydrodiferulic acid **7b**, Fig. 3, from maize bran insoluble fibre. This is the first isolation/characterisation of a saccharide-linked dehydrodimer other than the 5-5-dehydrodiferulate that was, until relatively recently (Ralph et al., 1994), the only known ferulate dehydrodimer. We speculate further on the nature of inter- and intra-molecular coupling of polysaccharide chains mediated by ferulates.

2. Results and discussion

2.1. Isolation of arabinosyl dehydrodiferulates

Owing to its high dehydrodiferulates content (Bunzel et al., 2001; Saulnier and Thibault, 1999), maize bran was chosen for the isolation of dehydrodiferuloyl saccharides. The conditions of acidic hydrolysis, optimised for the release of esterified ferulic acid with minimal release of free ferulic acid, have been detailed previously by Saulnier et al. (1995). Following a pre-separation step on Amberlite XAD-2, the fraction obtained by eluting with 50/50 methanol/water was selected to isolate dehydrodiferuloyl saccharides by Sephadex LH-20 chromatography. This fraction should contain dehydrodiferulic acids linked to low molecular mass saccharides. Using Sephadex LH-20 chromatography with aqueous or organic-aqueous eluents, separation of molecules is based not only on their molecular weight but also on interactions between the stationary phase and the phenolic compounds. A two step elution using water (which eluted feruloyl saccharides) and 20% aqueous methanol (which eluted dehydrodiferuloyl saccharides) gave a good separation of the two classes (Fig. 1). Isolation and structural determination of two major compounds eluted with water, 5-*O*-*trans*-feruloyl-L-arabinofuranose (fraction F**1**, Fig. 1; compound 1, Fig. 3) and *O*-β-D-xylopyranosyl-(1 → 2)-(5-*O*-*trans*-feruloyl-L-arabinofuranose) (fraction F**2**, Fig. 1; compound 2, Fig. 3) have been described by Saulnier et al. (1995). Five primary fractions, labelled **3**–**7** (Fig. 1), were obtained using

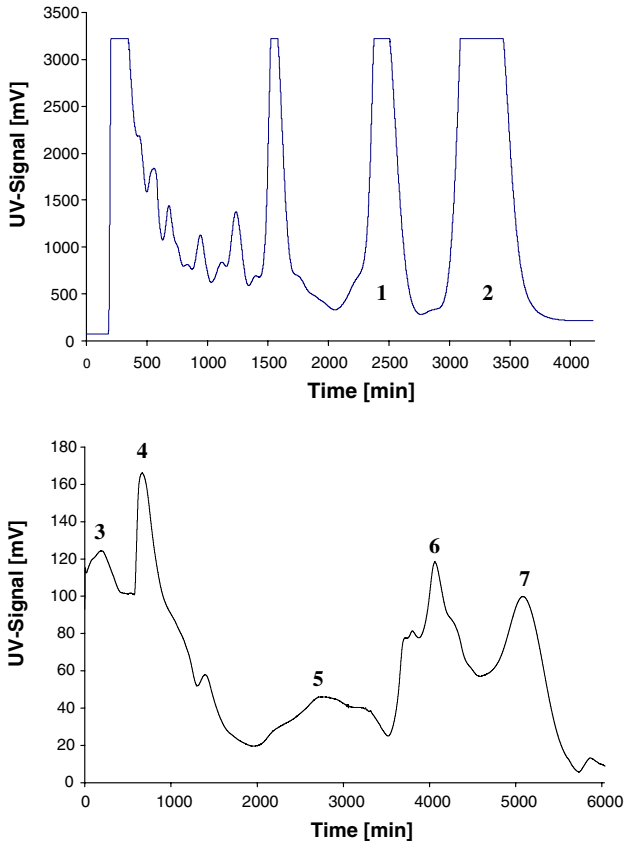

Fig. 1. Sephadex LH-20 chromatograms showing the separation of the acidic hydrolysates (MeOH/H_2O-fraction after Amberlite XAD-2 separation) using water (top) and methanol/water (20/80) (bottom) as eluents (detection at 325 nm).

20% methanol as eluent. Following saponification, phenolic compounds were determined to be associated with all five fractions by RP-HPLC. Relative retention times and UV-spectra were used for identification. None of the fractions contained a pure dehydrodiferuloyl saccharide, demonstrated by the release (by saponification) of at least two dehydrodiferulic acids from all fractions. The major phenolic compound derived from fraction **6** (F**6**) was 5-5-dehydrodiferulic acid. Fraction **7** (F**7**) produced a mixture of 5-5- and 8-*O*-4-dehydrodiferulic acids (ratio approximately 1:1). Both F**6** and F**7** were further purified/separated by semi-preparative RP-HPLC. Two fractions were obtained from F**7** (F**7a** and F**7b**) (Fig. 2). Purification of F**6** gave one major fraction (F**6p**, p-purified).

2.2. Structural identification of *F6p, F7a* and *F7b*

5-5-Dehydrodiferulic acid was the major phenolic compound identified after alkaline hydrolysis of F**6p** and F**7a**, whereas 8-*O*-4-dehydrodiferulic acid was the sole phenolic compound from F**7b**. Arabinose was the only carbohydrate released from F**7b**, determined as its alditol acetate after acidic hydrolysis. F**7a** contained arabinose and xylose and F**6p** a mixture of arabinose, xylose and galactose.

Further analysis of F**6p** (HPLC-MS, NMR) showed that this fraction was a complex mixture of different 5-5-dehydrodiferuloyl saccharides. No attempts at further separation were made. The molecular weight of F**7a** was 782 (potassium adduct ion with *m/z* 821 $[M + K]^+$ and sodium adduct ion with *m/z* 805 $[M + Na]^+$), consistent with one dehydrodiferulic acid and three pentose units. The structure of F**7a** was obtained, using one- and two-dimensional NMR experiments. It consists of 5-5-dehydrodiferulic acid, two arabinose and one xylose moieties, Fig. 3, and has been described previously (Saulnier et al., 1999).

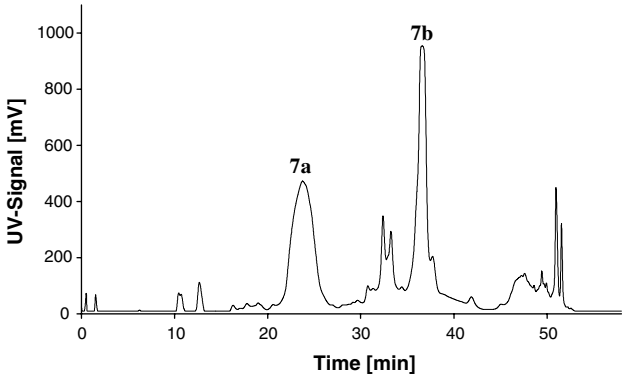

Fig. 2. Semi-preparative RP-HPLC-chromatogram obtained from fractionation of F**7** under conditions pertaining to the procedure described in Section 4.

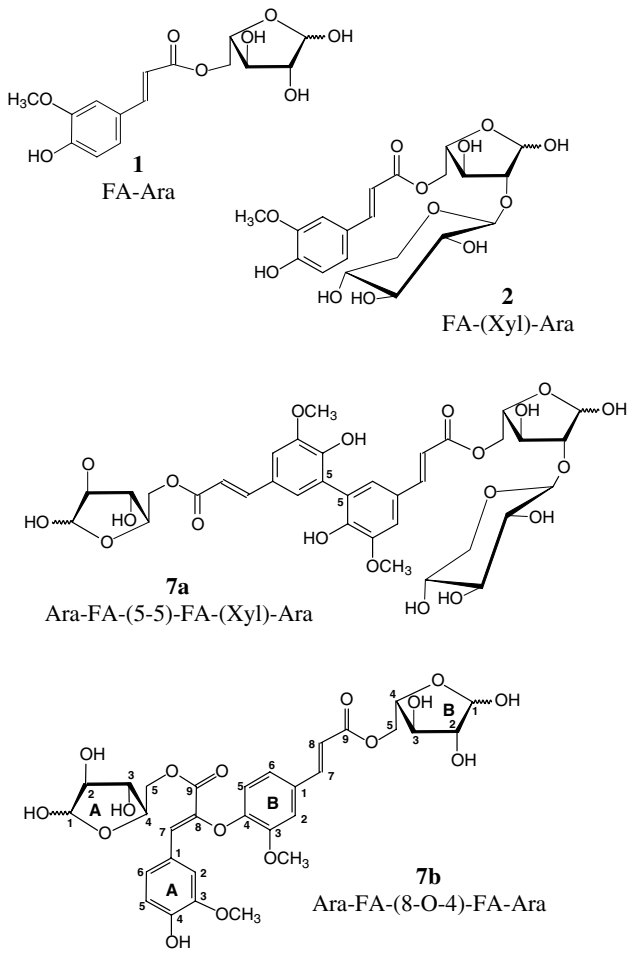

Fig. 3. Structure and numbering system of isolated feruloyl and dehydrodiferuloyl saccharides **1**, **2**, and **7a** (which have been previously identified) and **7b**, the di-5-*O*-L-arabinosyl ester of 8-*O*-4-dehydrodiferulate that is the main subject of this paper.

Analysis of F**7b** by HPLC-MS gave potassium adduct ion with *m/z* 689 $[M + K]^+$ and sodium adduct ion with *m/z* 673 $[M + Na]^+$, indicating a molecular mass of 650, corresponding to one dehydrodiferulic acid and two pentoses. High-resolution MS, found $[M + Na]^+$ 673.17516, $C_{30}H_{34}NaO_{16}$ requires M 673.17445. Preliminary analysis suggested that F**7b** was the elusive 8-*O*-4-dehydrodiferulate with each acid esterified by an arabinosyl unit. Although the quantity of 8-5-, 8-8-, and 8-*O*-4-dehydrodiferulates all typically exceed the amount of 5-5-dehydrodiferulate, it is only saccharide esters of the latter that have to date been isolated and characterised (Ishii, 1997). The main concern of this paper is therefore the structural elucidation of F**7b** by MS and NMR experiments.

The aromatic/double-bond region of the NMR spectrum, Fig. 4, is relatively easy to interpret. At least two sets of resonances, in approximately a 2:1 ratio, are seen for each proton due to their attachment to either the α- or the β-anomer of arabinose. The important **A**7 singlets

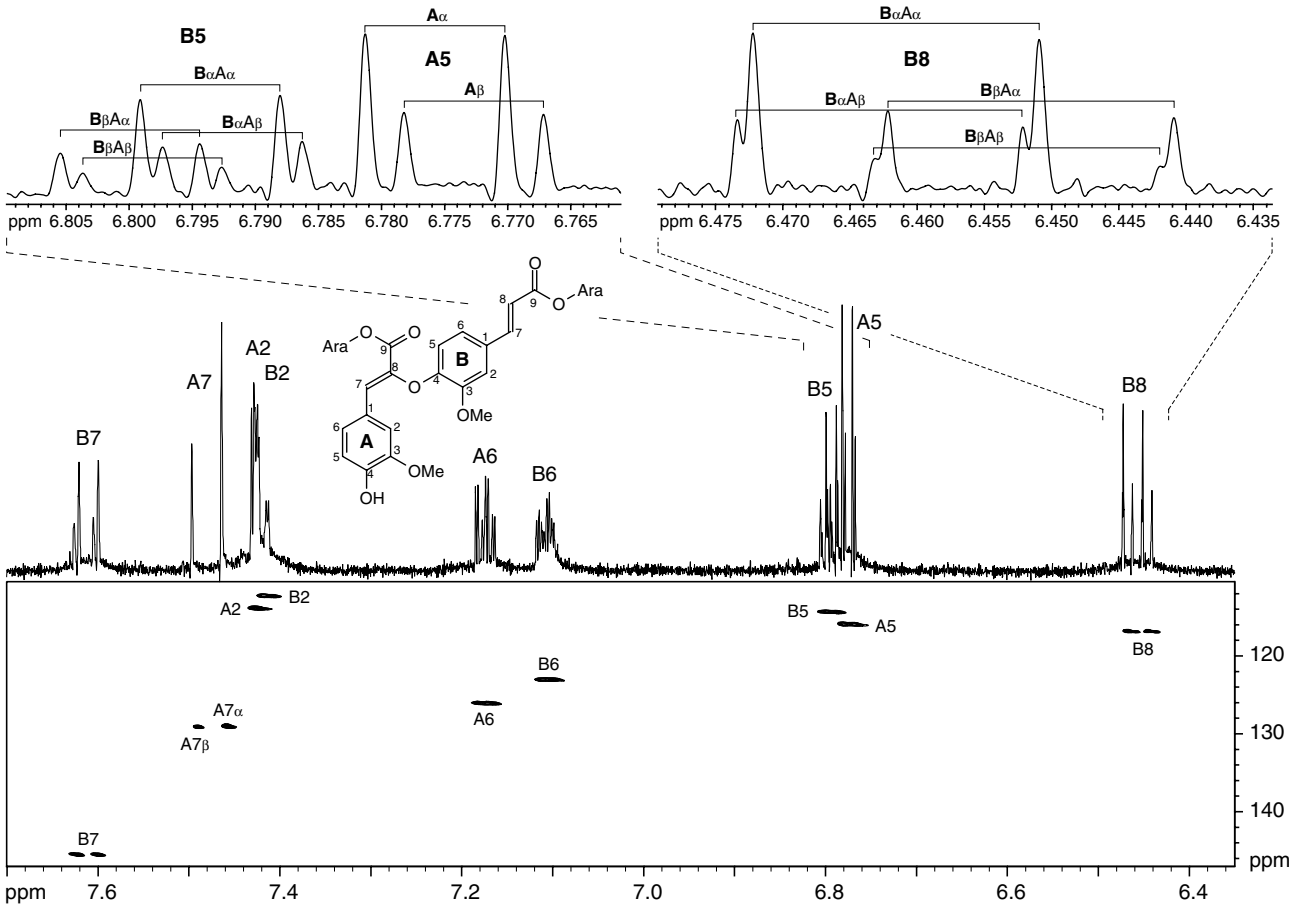

Fig. 4. Proton and HSQC spectra of the ferulate region of compound **7b**. The expanded proton regions show that, for some protons (notably **B**8 and **B**5), the entire four isomers (from two anomers of each arabinose unit) can be resolved. The expansions are labeled to signify the attached arabinose unit followed by the remote arabinose on the other moiety; thus **B**αAβ signifies a **B**-unit ferulate attached to the α-anomer of arabinose in a molecule in which the **A**-unit is esterified by an arabinose β-anomer. *Note*: non-ideal shim (producing baseline humps around the peaks and some tailing) was due in part to the use of volume-restricted NMR tubes.

are the prime indicators that moiety **A** is 8-*O*-linked; following 8-*O*-4-radical coupling, the intermediate quinone methide rearomatises by elimination of its acidic 8-proton (Ralph et al., 1994). Proton **A**7α is a singlet at 7.46 ppm whereas, **A**7β is a singlet of about half the height at about 7.50 ppm. Similarly, **A**5 is an 8.3 Hz doublet at 6.7755 ppm when attached to the α-anomer and 6.7725 ppm for the β-anomer. The **B**-ring protons experience the effect of both arabinose substituents. Proton **B**8 for example resolved into four 16.0 Hz doublets; the tallest is the one in which the **B**- and **A**-moiety arabinose substituents are both the predominant α-anomers (**B**αAα). At half the height, and just slightly higher chemical shift, is the doublet in which the **B**-unit is still esterified with an α-arabinose whereas the **A**-unit is esterified with the less predominant β-arabinose (**B**αAβ). At significantly lower chemical shift are the doublets in which the **B**-unit is esterified with a β-arabinose; the tallest, at half the height of the **B**αAα doublet and the same height as the **B**αAβ doublet is the **B**βAα doublet, while at half its height again is the **B**βAβ doublet. Similarly protons **B**5 resolved into four doublets in a similar way (expansion in Fig. 4, data in Table 1). Also, whereas **A**6 is a clean pair of doublet-of-doublets, one (with the attached β-arabinosyl unit) at half the height of the other (with the attached α-arabinosyl unit), the **B**6 protons are obviously more complex but again can be fully resolved into the four component doublets-of-doublets (expansion not shown but data presented in Table 1). Proton peaks are therefore in the typical ferulate guaiacyl pattern; their ready identification allows their carbons (data in Table 2) to be identified in the ^{13}C–^{1}H correlation (HSQC) experiment (Fig. 4).

NMR interpretation of the aliphatic arabinose region is made complex, even at 750 MHz, by the presence of four isomers here from the two anomers of each of the arabinose units. The anomeric protons of all four are almost completely resolved (Fig. 5(a)), the β-anomers at higher chemical shifts than the more dominant α-anomers, and the units attached to the **B**-unit at higher chemical shifts than those attached to the **A**-unit. The TOCSY experiment, Fig. 5(b), then

Table 1
^{1}H NMR data for compounds **7b**, the di-5-*O*-L-arabinosyl esters of 8-*O*-4-dehydrodiferulic acid (in acetone-d_6:D_2O 9:1); chemical shifts δ_H in ppm, coupling constants J in Hz

H		Arabinose moiety				Ferulate moiety					
		Aα	**A**β	**B**α	**B**β	**A**α	**A**β	**B**α**A**α	**B**α**A**β	**B**β**A**α	**B**β**A**β
1		5.102 $J_{1,2}$ = 2.06	5.197 $J_{1,2}$ = 4.51	5.135 $J_{1,2}$ = 2.25	5.202 $J_{1,2}$ = 4.13						
2		3.956 $J_{2,3}$ = 3.56	3.911 $J_{2,3}$ = 5.93	3.972 $J_{2,3}$ = 3.89	3.907 $J_{2,3}$ = 6.75	7.4297 $J_{2,6}$ = 2.1	7.4239 $J_{2,6}$ = 2.1	7.4259 $J_{2,6}$ = 2.1	7.4259 $J_{2,6}$ = 2.1	7.4136 $J_{2,6}$ = 2.1	7.4145 $J_{2,6}$ = 2.1
3		3.862 $J_{3,4}$ = 6.01	4.030 $J_{3,4}$ = 6.57	3.886 $J_{3,4}$ = 5.83	4.028 $J_{3,4}$ = 6.38						
4		4.169 $J_{4,5ax}$ = 5.99 $J_{4,5eq}$ = 3.47	3.883 $J_{4,5ax}$ = 7.05 $J_{4,5eq}$ = 3.48	4.192 $J_{4,5ax}$ = 6.72 $J_{4,5eq}$ = 3.53	3.866 $J_{4,5ax}$ = 6.40 $J_{4,5eq}$ = 3.73						
5	$\mathbf{5}_{ax}$	4.220 $J_{5ax,5eq}$ = −11.52	4.177 $J_{5ax,5eq}$ = −11.60	4.174 $J_{5ax,5eq}$ = −11.82	4.236 $J_{5ax,5eq}$ = −12.19	6.7755 $J_{5,6}$ = 8.3	6.7725 $J_{5,6}$ = 8.3	6.7935 $J_{5,6}$ = 8.3	6.7915 $J_{5,6}$ = 8.3	6.7995 $J_{5,6}$ = 8.3	6.7985 $J_{5,6}$ = 8.3
	$\mathbf{5}_{eq}$	4.362	4.314	4.330	4.333						
6						7.1778	7.1703	7.1105	7.1071	7.1051	7.1015
7						7.4640	7.4967	7.6102 $J_{7,8}$ = 16.0		7.6155 $J_{7,8}$ = 16.0	
8								6.4616	6.4628	6.4515	6.4525
OMe						3.673	3.670	3.96	3.96	3.96	3.96

Table 2
^{13}C NMR data for compounds **7b**, the di-5-*O*-L-arabinosyl esters of 8-*O*-4-dehydrodiferulic acid (acetone-d_6:D_2O 9:1); chemical shifts δ_C in ppm

C	Arabinose moiety				Ferulate moiety			
	Aα	**A**β	**B**α	**B**β	**A**α	**A**β	**B**α	**B**β
1	103.09	96.93	103.09	96.93	124.69	124.69	129.81	129.92
2	82.91	77.70	83.00	77.70	113.80	113.96	112.22	112.29
3	78.00	76.50	78.18	76.50	148.32	148.32	149.86	149.86
4	81.56	80.30	81.56	80.30	149.48	149.48	148.58	148.58
5	65.70	66.60	65.16	67.00	115.90	115.86	114.35	114.30
6					126.03	126.02	123.09	122.97
7					128.99	129.06	145.53	145.50
8					137.36	137.30	116.79	116.81
9					163.79	163.73	167.71	167.59
OMe					55.69	55.69	56.36	56.36

Data are from 2D HSQC and HMBC spectra; a 1D ^{13}C NMR spectrum was run but was to weak to deduce the peak detail.

identifies the proton coupling network for each. Determining the proton assignments requires the aid of the COSY experiment, Fig. 5(c), which is difficult to fully assign because of severe overlap, but allows most of the protons to be assigned and particularly distinguishes the 2- and 3-protons. The HSQC spectrum, Fig. 5(d), aids in the assignment of the 5-protons/carbons and provides the carbon chemical shifts. Nevertheless, there is significant overlap making unambiguous assignments difficult. Finally, the long-range correlation experiment (HMBC, not shown) allows assignment of the two rings (**A** vs **B**) since the carbonyl carbon resonances are well dispersed at 163.6 and 167.5 ppm (the latter matching well with FA–Ara at 169.8 ppm in D_2O (Bunzel et al., 2002), and 167.9 ppm in 9:1 acetone-d_6:D_2O (unpublished) which models the **B**-unit).

Much of the spectral assignment ambiguity was resolved by exploiting the extra dispersive power of a third dimension. The 3D TOCSY–HSQC experiment is particularly efficient, even finding considerable value for polymeric lignins (Marita et al., 2001; Ralph et al., 1999). Fig. 6(a) shows the 2D HSQC reference spectrum, along with f2–f3 planes at given proton shifts in which the two α-anomers are well isolated, and a combined β-anomers plane. These planes firmly identify the carbons belonging to each compound. Planes at given proton frequencies corresponding to each of the anomeric protons in the f1–f2 direction, Fig. 6(b), give beautiful HSQC–TOCSY correlation spectra isolating each of the four compounds, unambiguously revealing the proton data for even the two β-anomers where the anomeric protons are partially overlapping. Finally, f1–f3 planes at given carbon frequencies in the

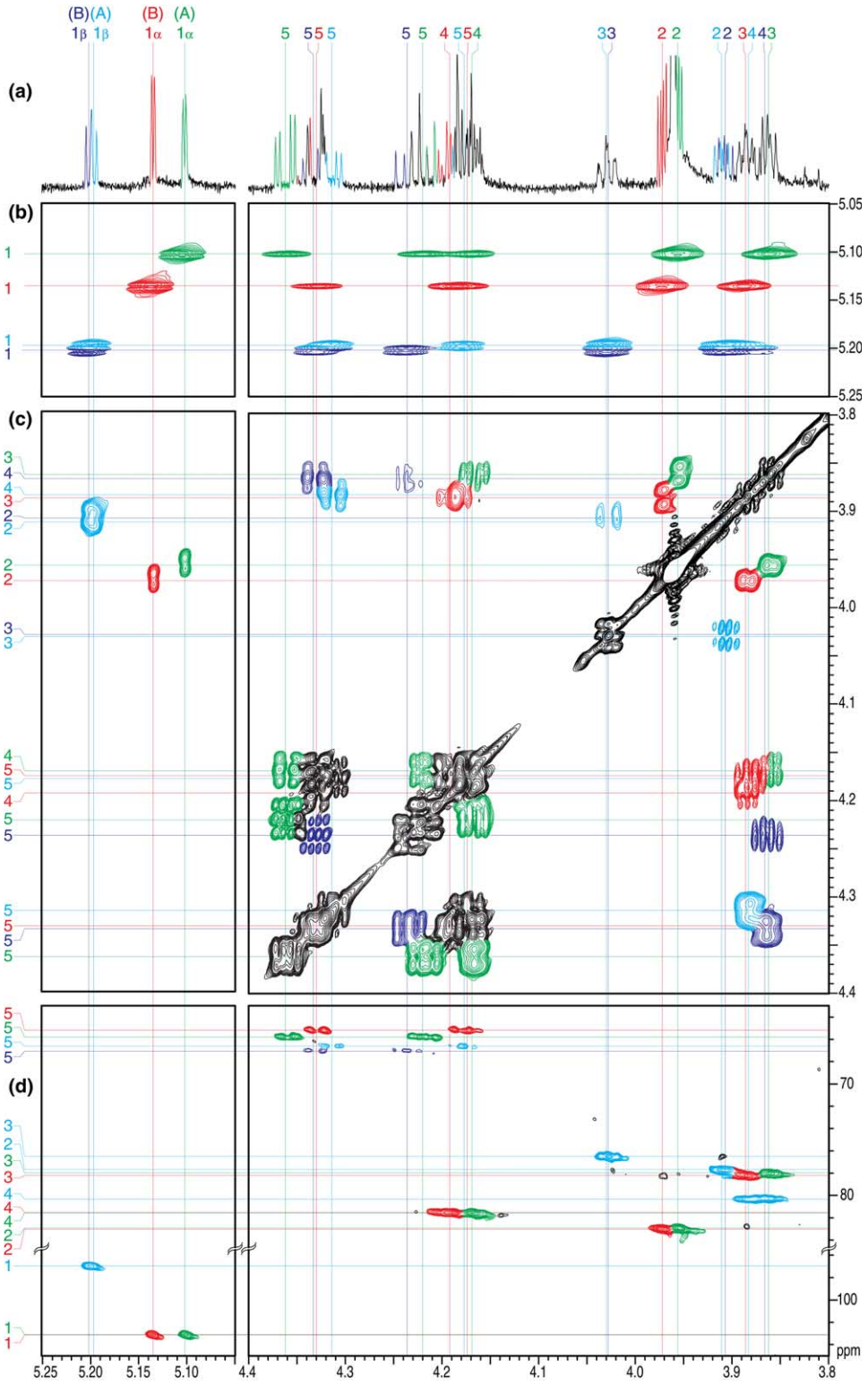

Fig. 5. Assignment of the arabinose regions. (a) Proton NMR spectrum (color-coded following the assignment process – see text). (b) TOCSY section showing correlations between the resolved anomeric protons and the other five protons in each arabinose coupling network. (c) COSY experiment which clarifies assignments of particularly the 2- and 3-protons. (d) HSQC experiment which clarifies the 5-proton assignments and yields ^{13}C chemical shifts for each unit (but which was difficult to resolve until the 3D experiment of Fig. 6).

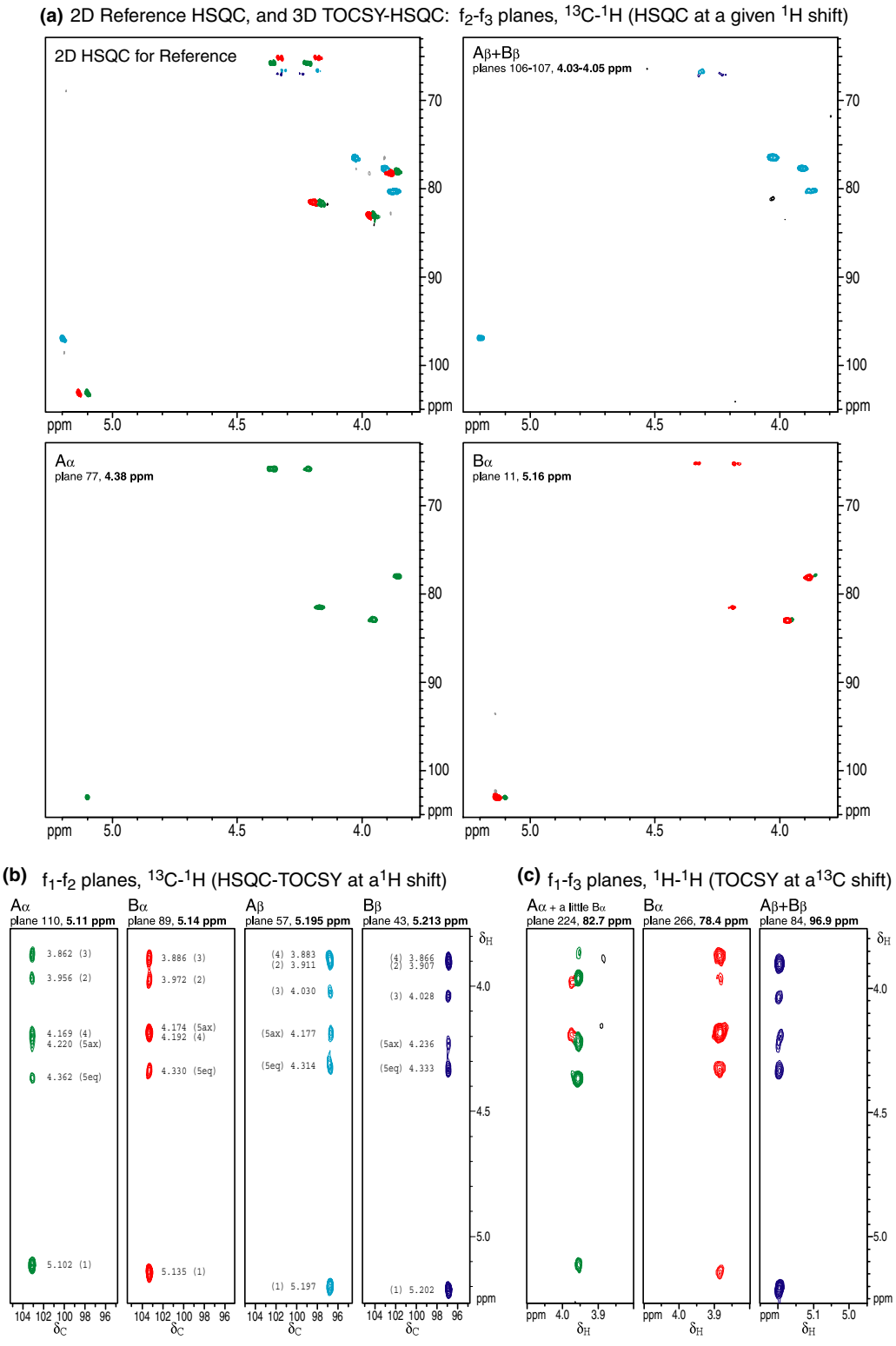

Fig. 6. Resolving the four arabinose units by 3D NMR. (a) A 2D HSQC spectrum for reference, followed by three ^{13}C–^{1}H (f2-f3) planes (at given proton shifts) that reasonably isolate each of the two α-arabinose units, and a combined plane with the β-units. (b) Four selected ^{13}C–^{1}H (f1-f2) HSQC–TOCSY planes (at the given ^{1}H shifts in the anomeric proton region) on which the four arabinose units are fully resolved. The deduced proton shifts (and assignments from the whole complement of experiments) are denoted beside each contour. (c) Three selected ^{1}H–^{1}H (f1–f3) TOCSY planes (at given ^{13}C shifts) on which the α-arabinose units are reasonably well resolved, and a plane on which the two β-units overlap (but is mainly Bβ). *Note*: when overlapped peaks/contours appear (especially for **B**β and **A**β), contours are simply colored as the more dominant one for simplicity.

remaining direction, Fig. 6(c), give fairly well resolved TOCSY spectra. The 3D experiment therefore nails down most chemical shift assignments for all of the four compounds.

The only remaining problem is to extract coupling constants and more precise chemical shifts, especially where signals are close to one another. The best way to deal with the complexity of this spectrum was to mathematically simulate the spectra for each isomer; spectral simulation provides the best chemical shift and coupling constant data when protons are tightly coupled. Chemical shifts were estimated from the

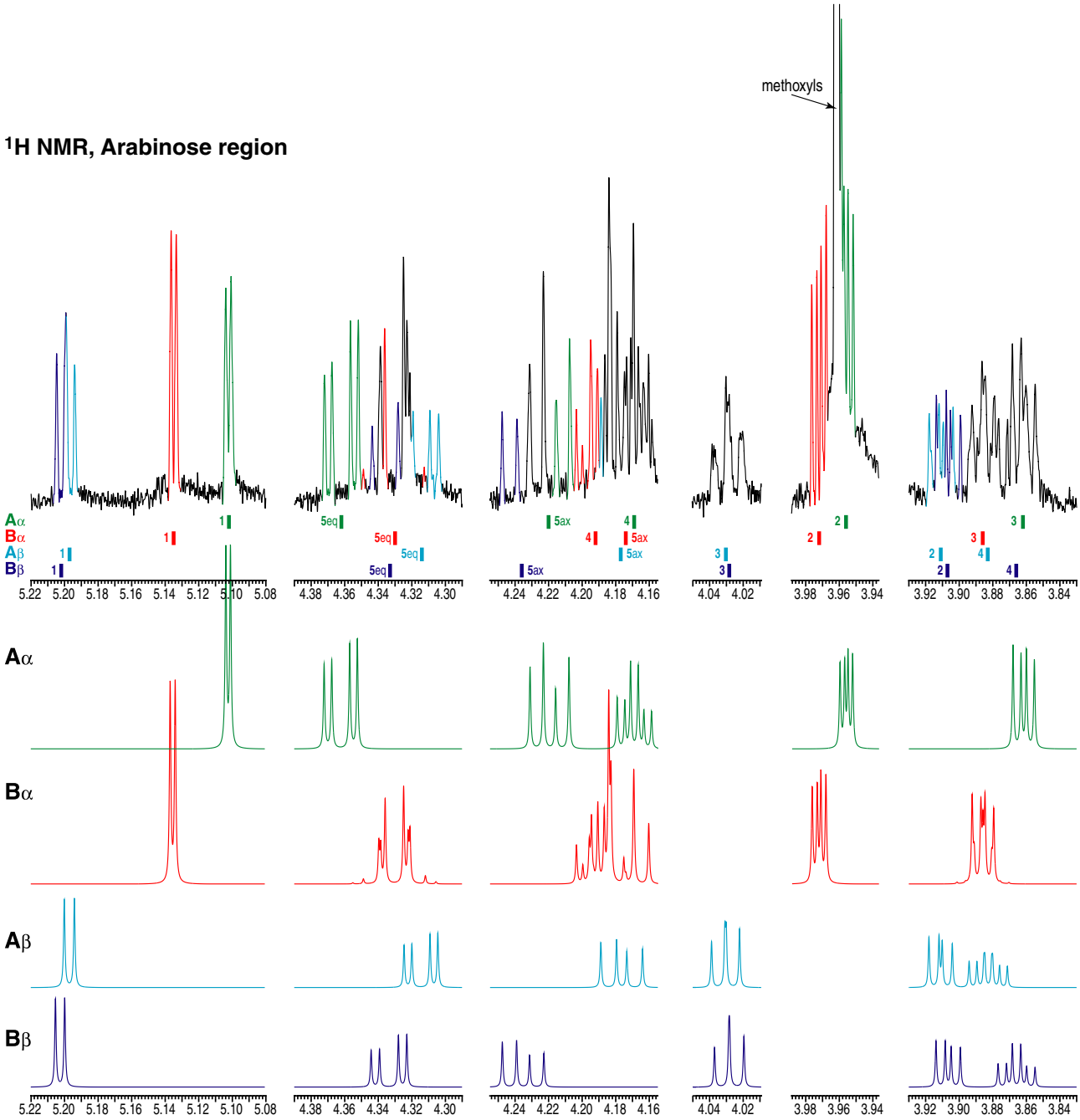

Fig. 7. Simulation of the arabinose unit proton spectra. The top trace is the measured 750 MHz spectrum, resolution enhanced. Our inability to brilliantly shim this sample in its restricted-volume Shigemi tube is clear from the tailing to the right of each peak, particularly noticeable from the strong methoxyls at 3.963 and 3.961 ppm. Peaks that have a definitely discernable origin are color coded for each arabinose anomer as in Fig. 5 and in the following plots. Actual chemical shifts are depicted along the bottom of the top plots. Below are the iteratively matched simulated spectra for each of the two anomers of each arabinose, color coded as in previous figures. The *ax* and *eq* descriptors denote the pseudo-axial (*proS*) and pseudo-equatorial (*proR*) assignments based on deuterium exchange studies from Serianni's group (Wu et al., 1983).

TOCSY, COSY, and HSQC experiments. As many of the coupling constants as possible were estimated from the 750 MHz ^{1}H NMR spectrum. In some cases, such as the doublet-of-doublets at ~4.36 ppm, patterns were obvious by inspection. In other cases, such as the eight line pattern centered at ~3.91 ppm and the six line pattern centered at ~4.225 ppm, two overlapping doublets-of-doublets can be uncovered by careful analysis. Where coupling constants could not be estimated from the spectrum, coupling constants from arabinose analogs were used. The spectrum for each arabinose isomer was calculated using these estimates as starting values. Peaks in the spectrum of each isomer were assigned to peak positions in the actual spectrum. The chemical shifts and coupling constants were varied and the spectrum recalculated until the peaks of the calculated spectrum duplicated peaks in the actual NMR spectrum. Comparisons between the calculated spectrum of each isomer and the actual NMR spectrum are shown in Fig. 7. In some cases, such as the 5*eq* multiplet of isomer **B**α (red), the non first order nature resulting from the tight coupling of the 4 and 5*ax* protons produces a pattern from which visual extraction of NMR data is clearly impossible. The chemical shifts and coupling constants used to calculate the final arabinose spectra are summarised in Tables 1 and 2.

All of the data are fully consistent with the compounds isolated being the four isomers of the di-5-*O*-L-arabinosyl ester of 8-*O*-4-dehydrodiferulic acid. The identification as an L-arabinose moiety was not proven here since the existence of arabinose units in grass arabinoxylans as their α-L-arabinosyl isomers is already well established (Ishii, 1997).

3. Conclusions

The capability of dehydrodiferulates to act as intra- and/or inter-molecular cross-linking agents in the plant cell walls has long been discussed (Fry, 1986; Hatfield et al., 1999; Ishii, 1997; Ralph et al., 1993, 1998, 2004). The isolation of 5-5-dehydrodiferuloyl saccharides (Ishii, 1991; Saulnier et al., 1999) provided the first conclusive structural evidence that dehydrodiferulates attach to two saccharide units. However, according to molecular modelling experiments both ferulate units of 5-5-coupled dehydrodiferulate, uniquely, may be tethered to the same arabinoxylan chain; the characterisation of the 5-5-coupled product does not therefore prove intermolecular cross-linking between different polysaccharide chains (Hatfield and Ralph, 1999). The diarabinosyl ester of 8-*O*-4-dehydrodiferulic acid is the first saccharide-linked dehydrodiferulate other than 5-5-dehydrodiferulate that has been isolated and characterised. Its existence provides the required evidence that dehydrodiferulates may act as intermolecular cross-linking agents in cell walls. Intermolecular cross-linking has profound effects on the structure of plant cell walls, influencing the physico-chemical and possibly physiological properties of cereal grain fibres in general. However, the mentioned molecular modelling study used a rather inflexible xylan backbone consisting of 16 xylose units. Due to the proposed semi-flexible structure of larger arabinoxylans we can not fully exclude the possibility of intramolecular formation of the 8-*O*-4-diferulate from two ferulates located at the opposite ends of the xylan chain.

4. Experimental

4.1. Plant materials

Maize bran (*Zea mays* L.) was kindly provided by Hammermühle Maismühle GmbH (Kirrweiler, Germany).

4.2. General

Heat-stable α-amylase Termamyl 120 L (EC 3.2.1.1, from *Bacillus licheniformis*, 120 KNU/g) was from Novo Nordisk (Bagsvaerd, Denmark). Amberlite XAD-2 was obtained from Serva (Heidelberg, Germany), and Sephadex LH-20 was from Pharmacia Biotech (Freiburg, Germany). Methanol (MeOH) (HPLC grade) was from Baker (Deventer, Holland), acetone-d_6 was from Isotec (Miamisburg, OH, USA), and deuterium oxide from Sigma (Milwaukee, WI, USA). All other chemicals and solvents were purchased from Merck (Darmstadt, Germany).

4.3. Preparation of insoluble maize fibre

n-Hexane defatted maize bran (20 g, milled to a particle size smaller than 0.5 mm) was suspended in phosphate buffer (pH 6.0, 0.08 M, 300 ml), and heat-stable α-amylase (1.5 ml) was added. Beakers were placed in a boiling water bath for 40 min and shaken every 5 min. After cooling down to room temperature, the suspension was centrifuged, and the residue was washed two times with hot water (70 °C), 95% ethanol and acetone, and was finally dried at 40 °C overnight in a vacuum oven. This procedure was performed several times.

4.4. Chemical degradation of insoluble fibre

Chemical degradation of insoluble fibre was carried out as described previously (Bunzel et al., 2002; Saulnier et al., 1995) but with minor modifications. Insoluble fibre (55 g) was treated with 50 mM trifluoroacetic acid (1.2 l) under reflux for 3 h at 100 °C. After centrifugation the supernatant was filtered and evaporated at

40 °C under vacuum to 200 ml. The solution was adjusted to pH 5.0 using 0.1 M NaOH and centrifuged again. Finally, the solution was concentrated to 100 ml.

4.5. Isolation of dehydrodiferuloyl oligosaccharides

The hydrolysate was applied to a column (40 × 5 cm) of Amberlite XAD-2. Elution was carried out with H_2O (1.5 l), MeOH/H_2O 50/50 (2 l) and MeOH (1.5 l). The MeOH/H_2O fraction was concentrated to 25.5 ml and applied to a column (100 × 3.2 cm) of Sephadex LH-20. A two step elution was performed: (1) elution with water for 70 h, flow rate: 1 ml min^{-1} (L-6000 pump, Merck/Hitachi, Darmstadt, Germany); (2) elution with MeOH/H_2O 20/80 (v/v) for 100 h, flow rate: 1 ml min^{-1}. The absorbance of the eluent was monitored continuously at 325 nm with an UV-detector equipped with a preparative flow cell (L-7400, Merck/Hitachi, Darmstadt, Germany). Fractions were collected every 18 min. Further purification of the isolated fractions was performed by semi-preparative HPLC (L-6200 Intelligent pump, Merck/Hitachi, Darmstadt, Germany) using a Nucleosil 100-5 C18 HD column (250 × 10 mm, 5 μm, Macherey-Nagel, Düren, Germany). Elution was carried out at room temperature and a flow rate of 4 ml min^{-1} was maintained. An acetonitrile/H_2O gradient was used: initially acetonitrile/H_2O 20/80, linear over 30 min to acetonitrile/H_2O 40/60, held isocratically for 10 min, followed by a rinsing and equilibration step. The injection volume was 50 μl using a 100 μl injection loop. Phenolic compounds were detected using an UV-detector (325 nm, Variable Wavelength Monitor 2141, LKB/Pharmacia, Freiburg, Germany).

4.6. Identification of dehydrodiferuloyl oligosaccharides

Phenolic compounds were determined by HPLC (L-6200 Intelligent pump, T-6300 Column thermostat, Merck/Hitachi, Darmstadt, Germany) using a Nucleosil 100-5 C18 HD column (250 × 3 mm, 5 μm, Macherey-Nagel, Düren, Germany) after alkaline hydrolysis. About 0.1–0.2 mg of purified fractions were saponified with NaOH (1 M, 200 μl, degassed with N_2) by stirring for 2 h in the dark at room temperature. The reaction was stopped by adding 2 M H_3PO_4 (150 μl). This solution was used directly for HPLC analysis. Elution was carried out using a gradient of aqueous 1 mM trifluoroacetic acid (TFA) and MeOH: initially MeOH/1 mM TFA 20/80, held for 10 min, linear over 5 min to MeOH/1 mM TFA 35/65, held isocratically for 15 min, linear over 10 min to MeOH/1 mM TFA 45/55, held for 10 min, followed by a rinsing and equilibration step. The injection volume was 20 μl, the column temperature 45 °C, and the flow rate was maintained at 0.8 ml min^{-1}. Phenolic compounds were detected using a Waters 994 programmable photodiode array detector (Waters, Eschborn, Germany) at 325 and 280 nm. Dehydrodiferulic acids were identified by comparison of their relative retention times and UV-spectra with those of authentic standard compounds (Bunzel et al., 2004).

Molecular weights of isolated dehydrodiferuloyl oligosaccharides were determined using HPLC-MS working in the positive-ion mode (HP Series 1100: autosampler G1313A, binary pump G1312A, degasser G1322A, mass spectrometer G1946A (ion-source: atmospheric pressure electro-spray ionisation), Hewlett–Packard, Waldbronn, Germany). Fast elution was carried out using a Nucleosil 100-5 C18 HD column (250 × 3 mm, 5 μm, Macherey-Nagel, Düren, Germany) and a gradient of ammonium formate buffer (pH 3) and acetonitrile: initially acetonitrile/ammonium formate 15/85 held for 2 min, linear over 5 min to acetonitrile/ammonium formate 50/50, held isocratically for 5 min. The injection volume was 20 μl, the column temperature 40 °C, and the flow rate was maintained at 0.7 ml min^{-1}. High-resolution mass spectrometry was performed on a MAT95XL (ThermoFinnigan MAT, Bremen, Germany) instrument, working in the positive ion mode.

Neutral carbohydrate compounds were determined as alditol acetates after acidic hydrolysis (2 M TFA, 120 °C, 60 min) by GLC (Hewlett–Packard 5890 Series II, Waldbronn, Germany). Reduction and acetylation was carried out as described elsewhere (Blakeney et al., 1983). Alditol acetates were separated using a HP-5MS capillary column (0.25 mm × 30 m × 0.25 μm film thickness) (Hewlett–Packard, Waldbronn, Germany). GLC conditions were as follows: initial column temperature: 45 °C, held for 1 min, ramped at 40 °C min^{-1} to 165 °C, held for 12 min, ramped at 10 °C min^{-1} to 220 °C, held for 3 min, ramped at 20 °C min^{-1} to 240 °C and held for 3 min; cold on-column injection, flame ionisation detection (detector temperature 300 °C). He (1.5 ml min^{-1}) was used as carrier gas.

1D and 2D NMR-spectra were acquired on a Bruker DMX-750 instrument (Karlsruhe, Germany) fitted with a 5-mm triple-resonance (^1H, ^{13}C, ^{15}N) gradient inverse probe (proton coils closest to the sample). Carbon/proton designations are based on conventional numbering (see structures in Fig. 3). The sample, ~2 mg, was dissolved in 0.5 ml of 9:1 acetone-d_6:D_2O; the central acetone solvent peak was used as internal reference (δ_H 2.04, δ_C 29.80). Experiments used were standard Bruker implementations of gradient-selected versions of inverse (^1H-detected) homonuclear correlation spectroscopy (COSY), total correlation spectroscopy (TOCSY), heteronuclear single quantum coherence (HSQC, HSQC–TOCSY), and heteronuclear multiple bond correlation (HMBC) experiments; the HMBC experiments used an 80 ms long-range coupling delay. The 3D experiment was run on a Bruker DMX-600 instrument (Karlsruhe, Germany) fitted with a 5-mm triple-resonance (^1H, ^{13}C, ^{15}N) gradient inverse cryoprobe for enhanced sensi-

tivity. The 3D gradient-selected TOCSY–HSQC experiment was trivially modified to use f2 as the carbon channel from "mleiietf3gs3d" (a 3 channel experiment using nitrogen on f3). The TOCSY spin lock period was 190 ms (optimised from a series of 2D TOCSY experiments). The experiment consisted of acquiring 512 real-time proton data points (f3) over a sweep width of 1.5 ppm, with 128 increments over 52 ppm in the carbon dimension (f2), and a further 32 increments over 1.5 ppm in the additional proton dimension (f1). The number of scans per increment was 16, the acquisition time was 0.285 s and a relaxation delay of 1 s was used; the experiment required 26.75 h to acquire. The spectrum was processed rather traditionally as a $1K \times 512 \times 128$ matrix, using Gaussian apodisation in f3, sine bell squared in f2 and f1, and minimal forward linear prediction.

1D proton chemical shifts and coupling constants were accurately determined by full spectral simulation using gNMR 3.6 for MacOS (Cherwell Scientific Publishing, Oxford, UK), as described in the text.

Acknowledgements

The authors thank the Deutsche Forschungsgemeinschaft (DFG) (Graduiertenkolleg 464 "Glycoconjugate" (University of Hamburg)) for financial support. We also are grateful to the CSREES-USDA-NRI competitive grants program (Grant No. 2003-01246), for partial funding. NMR experiments on the Bruker DMX-600 cryoprobe system and the DMX-750 were carried out at the National Magnetic Resonance Facility at Madison with support from the NIH Biomedical Technology Program (RR02301) and additional equipment funding from the University of Wisconsin, NSF Academic Infrastructure Program (BIR-9214394), NIH Shared Instrumentation Program (RR02781, RR08438), NSF Biological Instrumentation Program (DMB-8415048), and the US Department of Agriculture.

References

Blakeney, A.B., Harris, P.J., Henry, R.J., Stone, B.A., 1983. A simple and rapid preparation of alditol acetates for monosaccharide analysis. Carbohydr. Res. 113, 291–299.

Bunzel, M., Ralph, J., Marita, J., Steinhart, H., 2000. Identification of 4-*O*-5′-coupled diferulic acid from insoluble cereal fiber. J. Agric. Food Chem. 48, 3166–3169.

Bunzel, M., Ralph, J., Marita, J.M., Hatfield, R.D., Steinhart, H., 2001. Diferulates as structural components in soluble and insoluble cereal dietary fibre. J. Sci. Food Agric. 81, 653–660.

Bunzel, M., Allerdings, E., Sinnwell, V., Ralph, J., Steinhart, H., 2002. Cell wall hydroxycinnamates in wild rice (*Zizania aquatica* L.) insoluble dietary fibre. Eur. Food Res. Technol. 214, 482–488.

Bunzel, M., Ralph, J., Funk, C., Steinhart, H., 2003. Isolation and identification of a ferulic acid dehydrotrimer from saponified maize bran insoluble fiber. Eur. Food Res. Technol. 217, 128–133.

Bunzel, M., Funk, C., Steinhart, H., 2004. Semipreparative isolation of dehydrodiferulic and dehydrotriferulic acids as standard substances from maize bran. J. Sep. Sci. 27, 1080–1086.

Deetz, D.A., Jung, H.J., Helm, R.F., Hatfield, R.D., Ralph, J., 1993. Impact of methyl 5-*O*-(*E*)-feruloyl-α-L-arabinofuranoside on in-vitro degradation of cellulose and xylan. J. Sci. Food Agric. 61, 423–427.

Eraso, F., Hartley, R.D., 1990. Monomeric and dimeric phenolic constituents of plant cell walls – possible factors influencing wall biodegradability. J. Sci. Food Agric. 51, 163–170.

Fry, S.C., 1986. Cross-linking of matrix polymers in the growing cell walls of angiosperms. Ann. Rev. Plant Physiol. 37, 165–186.

Grabber, J.H., Hatfield, R.D., Ralph, J., 1998a. Diferulate cross-links impede the enzymatic degradation of non-lignified maize walls. J. Sci. Food Agric. 77, 193–200.

Grabber, J.H., Ralph, J., Hatfield, R.D., 1998b. Ferulate cross-links limit the enzymatic degradation of synthetically lignified primary walls of maize. J. Agric. Food Chem. 46, 2609–2614.

Hatfield, R.D., Ralph, J., 1999. Modelling the feasibilty of intramolecular dehydrodiferulate formation in grass walls. J. Sci. Food Agric. 79, 425–427.

Hatfield, R.D., Ralph, J., Grabber, J.H., 1999. Cell wall cross-linking by ferulates and diferulates in grasses. J. Sci. Food Agric. 79, 403–407.

Ishii, T., 1991. Isolation and characterization of a diferuloyl arabinoxylan hexasaccharide from bamboo shoot cell-walls. Carbohydr. Res. 219, 15–22.

Ishii, T., 1997. Structure and functions of feruloylated polysaccharides. Plant Sci. 127, 111–127.

Kamisaka, S., Takeda, S., Takahashi, K., Shibata, K., 1990. Diferulic and ferulic acid in the cell-wall of *Avena* coleoptiles – their relationships to mechanical properties of the cell-wall. Physiol. Plantarum 78, 1–7.

Marita, J.M., Ralph, J., Lapierre, L., Jouanin, L., Boerjan, W., 2001. NMR characterization of lignins in poplar altered in caffeic acid *O*-methyltransferase (COMT) activity. J. Chem. Soc., Perkin Trans. 1, 2939–2945.

Parr, A.J., Waldron, K.W., Ng, A., Parker, M.L., 1996. The wall-bound phenolics of Chinese water chestnut (*Eleocharis dulcis*). J. Sci. Food Agric. 71, 501–507.

Parr, A.J., Ng, A., Waldron, K.W., 1997. Ester-linked phenolic components of carrot cell walls. J. Agric. Food Chem. 45, 2468–2471.

Ralph, J., Hatfield, R.D., Quideau, S., Helm, R.F., 1993. Lignin cross-linking in the plant cell wall; unambiguous methods for identification, and structural/regiochemical characterization of cross-linked structures. In: NMR of Biomaterials Symposium, Am. Chem. Soc. Natl. Mtg., ACS, Denver, CO, pp. Cell-137.

Ralph, J., Quideau, S., Grabber, J.H., Hatfield, R.D., 1994. Identification and synthesis of new ferulic acid dehydrodimers present in grass cell-walls. J. Chem. Soc., Perkin Trans. 1, 3485–3498.

Ralph, J., Grabber, J.H., Hatfield, R.D., 1995. Lignin-ferulate cross-links in grasses: active incorporation of ferulate polysaccharide esters into ryegrass lignins. Carbohydr. Res. 275, 167–178.

Ralph, J., Hatfield, R.D., Grabber, J.H., Jung, H.G., Quideau, S., Helm, R.F., 1998. Cell wall cross-linking in grasses by ferulates and diferulates. In: Lewis, N.G., Sarkanen, S. (Eds.), Lignin and Lignan Biosynthesis, ACS Symposium Series, vol. 697. American Chemical Society, Washington, DC, pp. 209–236.

Ralph, J., Marita, J.M., Ralph, S.A., Hatfield, R.D., Lu, F., Ede, R.M., Peng, J., Quideau, S., Helm, R.F., Grabber, J.H., Kim, H., Jimenez-Monteon, G., Zhang, Y., Jung, H.-J.G., Landucci, L.L., MacKay, J.J., Sederoff, R.R., Chapple, C., Boudet, A.M., 1999. Solution-state NMR of lignins. In: Rials, T. (Ed.), Advances in Lignocellulosics Characterization. TAPPI Press, Atlanta, GA, pp. 55–108.

Ralph, J., Bunzel, M., Marita, J.M., Hatfield, R.D., Lu, F., Kim, H., Schatz, P.F., Grabber, J.H., Steinhart, H., 2004. Peroxidase-dependent cross-linking reactions of *p*-hydroxycinnamates in plant cell walls. Phytochem. Rev. 3, 79–96.

Rouau, X., Cheynier, V., Surget, A., Gloux, D., Barron, C., Meudec, E., Louis-Montero, J., Criton, M., 2003. A dehydrotrimer of ferulic acid from maize bran. Phytochemistry 63, 899–903.

Saulnier, L., Vigouroux, J., Thibault, J.F., 1995. Isolation and partial characterization of feruloylated oligosaccharides from maize bran. Carbohydr. Res. 272, 241–253.

Saulnier, L., Crepeau, M.J., Lahaye, M., Thibault, J.F., Garcia-Conesa, M.T., Kroon, P.A., Williamson, G., 1999. Isolation and structural determination of two 5,5′-diferuloyl oligosaccharides indicate that maize heteroxylans are covalently cross-linked by oxidatively coupled ferulates. Carbohydr. Res. 320, 82–92.

Saulnier, L., Thibault, J.F., 1999. Ferulic acid and diferulic acids as components of sugar-beet pectins and maize bran heteroxylans. J. Sci. Food Agric. 79, 396–402.

Tan, K.S., Hoson, T., Masuda, Y., Kamisaka, S., 1992. Involvement of cell wall-bound diferulic acid in light-induced decrease in growth-rate and cell-wall extensibility of *Oryza* coleoptiles. Plant Cell Physiol. 33, 103–108.

Waldron, K., 1998. Gemüse im Härtetest – Das Geheminis der chinesischen Wassernuß. Lebensmitteltechnik 30, 50–51.

Waldron, K.W., Ng, A., Parker, M.L., Parr, A.J., 1997. Ferulic acid dehydrodimers in the cell walls of *Beta vulgaris* and their possible role in texture. J. Sci. Food Agric. 74, 221–228.

Wu, G.D., Serianni, A.A., Barker, R., 1983. Stereoselective deuterium exchange of methylene protons in methyl tetrofuranosides: hydroxymethyl group conformations in methyl pentofuranosides. J. Org. Chem. 48, 1750–1757.

Zarra, I., Sanchez, M., Queijeiro, E., Pena, M.J., Revilla, G., 1999. The cell wall stiffening mechanism in *Pinus pinaster* Aiton: regulation by apoplastic levels of ascorbate and hydrogen peroxide. J. Sci. Food Agric. 79, 416–420.